

Hawking radiation with dispersion: the broadened horizon paradigm

Antonin Coutant*

Max Planck Institute for Gravitational Physics, Albert Einstein Institute, Am Mühlenberg 1, 14476 Golm, Germany, EU

Renaud Parentani†

Laboratoire de Physique Théorique, CNRS UMR 8627,
Bâtiment 210, Université Paris-Sud 11, 91405 Orsay Cedex, France

(Dated: February 12, 2014)

We study the spatial properties of the modes responsible for the Hawking effect in the presence of high frequency dispersion. Near the horizon, the modes are regularized on a small distance which only depends on the surface gravity and the scale of dispersion. The regularization explains why the spectrum is hardly affected by dispersion as long as the background geometry does not significantly vary over this composite length. For relevant frequencies, the regularization differs from the usual WKB resolution of wave singularity near a turning point. The latter only applies when the frequency is so high that the Hawking effect is negligible.

INTRODUCTION

For relativistic fields, the stationary modes ϕ_ω responsible for the Hawking effect possess a singular behavior on the horizon. Namely, for $|x| \rightarrow 0$, one finds

$$\phi_\omega \propto |x|^{i\omega/\kappa}, \quad (1)$$

where ω/κ is their Killing frequency in the unit of the surface gravity, and where x is the proper distance from the horizon measured in a freely falling frame. As Eq. (1) is found irrespectively of the mass and the orbital momentum, we can and shall work with massless 1 + 1 dimensional fields. The stationary geometry shall be described by the line element

$$ds^2 = dt^2 - (dx - v(x)dt)^2, \quad (2)$$

where t is the proper time along the freely falling orbits $dx = vdt$, with $v < 0$. The horizon is located at $v^2 = 1$, and in its vicinity, one has $v = -1 + \kappa x$. The interior of the black hole, $|v| > 1$, is thus $x < 0$.

As understood by Unruh [1], the singular behavior of Eq. (1) unambiguously fixes the temperature of the emitted radiation. Indeed, the regularity of the state across the horizon fixes the ratio of the coefficients weighing ϕ_ω on either side of $x = 0$. This in turn fixes the temperature to be the Hawking one [2]: $T_H = \kappa/2\pi$ in units where $c = \hbar = k_B = 1$. Notice finally that the regularity across the horizon is efficiently implemented by working in Fourier space with modes that contain only positive wave vector $p = -i\partial_x$ [3, 4]. Importantly, when including short distance dispersion [5], it is still convenient to work in the p -representation [6], as we shall see below.

From Eq. (1) one sees that the freely falling frequency

$$\Omega = \omega - vp \sim p \sim \frac{\omega}{\kappa x}, \quad (3)$$

increases without bound as $x \rightarrow 0$. This blueshift connects the infrared physics of the low wave number $p \sim \kappa$,

to deep ultraviolet physics where the assumption of free field in classical background might break down. This raises the *transplanckian question* [7, 8], namely to what extent the predictions derived from Eq. (1) actually depend on the short distance behavior of the theory.

In analog models [5, 9, 10], this question can be addressed explicitly since for short wavelengths, one leaves the hydrodynamical (effectively relativistic) regime for some dispersive regime. To characterize the first deviations, we shall consider

$$\Omega^2 = F^2(p) = p^2(1 - p^2/\Lambda^2). \quad (4)$$

The minus sign means that the dispersion is subluminal (the superluminal case can be treated in a similar way, see Sec.III.E in [11]). Λ defines the momentum scale above which Lorentz invariance ceases to be valid. Its value is determined by the microscopic structure of the medium. Since [5], attention has been mainly given to the modifications of the asymptotic spectrum due to high momentum dispersion [6, 11–16]. In this paper instead, we consider the near horizon properties of the dispersive modes. As could have been expected, short distance dispersion regularizes the logarithmic divergence of Eq. (1), see in particular [17]. Depending on the value of ω/κ , we found that the dispersive modes follow two very distinct behaviors. Nevertheless both involve the same ω -independent composite length scale. Interestingly, this length scale was previously found in numerical analysis of dispersive spectra [14, 15]. Our treatment therefore provides a rational explanation for these numerical observations.

NEAR HORIZON BEHAVIOR

We consider a massless field propagating in the geometry of Eq. (2) and obeying the dispersion relation (4). At fixed ω , the mode ϕ_ω obeys [5, 6]

$$[(\omega + i\partial_x v)(\omega + iv\partial_x) - F^2(-i\partial_x)]\phi_\omega = 0. \quad (5)$$

Close to the horizon, one has $v \sim -1 + \kappa x$. This approximation is valid only for a finite range of x , that we call x_{lin} . In familiar black hole geometries (such as Schwarzschild), x_{lin} is of the order of $1/\kappa$. Yet, in some media, it might be much smaller, and this significantly affects the spectrum [16]. x_{lin} is the first relevant length of the problem.

The first manifestations of short distance dispersion can be seen in geometrical optics, at the level of the characteristics of Eq. (5), solutions of $(\omega - vp)^2 = F^2(p)$. Interestingly, the equation for the wave number, $dp/dt = -(\partial x/\partial \omega)^{-1}$, is unaffected by dispersion in the near horizon region, and its solution is still $p = p_0 e^{-\kappa t}$ [9]. Instead, the solutions of $dx/dt = (\partial p/\partial \omega)^{-1}$, critically depend on F . When considered backwards in time, the characteristics are swept away from the horizon at short wavelengths, see Fig. 1. Depending on the sign of Ω , two types of trajectories exist. For ω and Ω positive, the characteristic first approaches the horizon with $x > 0$ as p increases. Then at the value $p_{\text{tp}} = \omega^{1/3} \Lambda^{2/3}$, it bounces back away from the horizon. The locus of the turning point is

$$x_{\text{tp}}(\omega) = \frac{3\omega}{2\kappa} \frac{1}{p_{\text{tp}}} = \frac{3}{2\kappa} \left(\frac{\omega}{\Lambda}\right)^{2/3}. \quad (6)$$

This expression is valid if x_{tp} lies within the near horizon region, i.e., $x_{\text{tp}} \ll x_{\text{lin}}$. Eq. (6) gives the first composite length of the problem. For $\omega > 0$ but $\Omega < 0$, one obtains the trajectory followed by the negative energy ‘‘partner’’. It focuses on the horizon from the left, crosses the horizon, and follows the $\Omega > 0$ characteristic.

We just saw that the description of the characteristics is much simpler in p -space than in x -space. When abandoning geometrical optics, this is again true. In the near horizon region, using $\hat{v} = -1 + i\kappa \partial_p$, one finds that the solution of Eq. (5) factorizes in a peculiar form [6]

$$\tilde{\phi}_\omega(p) = \frac{p^{-i\frac{\omega}{\kappa} - 1}}{\sqrt{2\pi}} \times \chi(p) e^{-i\frac{p}{\kappa}}. \quad (7)$$

The first factor is the relativistic mode. Indeed the Fourier transform of Eq. (1) gives $|p|^{-i\omega/\kappa - 1}$. The function χ obeys a ω -independent second order equation

$$-\kappa^2 p^2 \partial_p^2 \chi = F^2(p) \chi. \quad (8)$$

These simplifications are directly related to an extra de Sitter symmetry¹. To solve Eq. (8), we use the

¹ In fact, when considered globally, $v = -1 + \kappa x$ corresponds to de Sitter space. This geometry possesses extra symmetries with respect to a stationary black hole metric. Importantly, one of them is compatible with the existence of preferred (freely falling) frame [18]. Therefore, de Sitter endowed with such a frame offers a simple specific dispersive model. It allows to explicitly compute the modes and the spectrum [18].

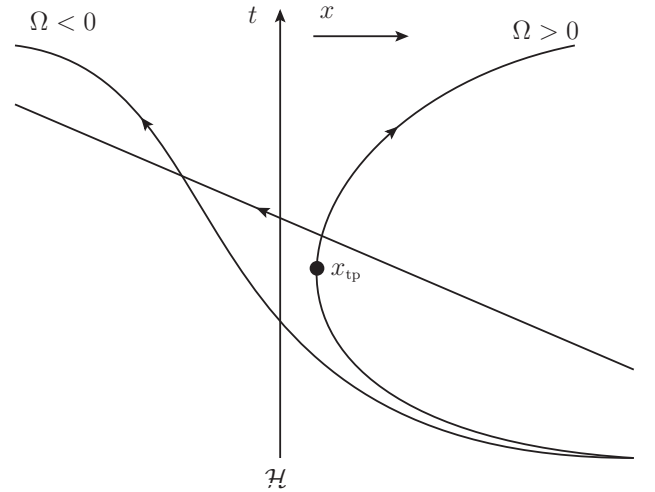


Figure 1. Space-time structure of characteristics in the near horizon region, with positive (right side) and negative (left) freely falling frequency $\Omega = \omega - vp$. At large times, both follow some null outgoing geodesic, $dx = (1+v)dt$, see Eq. (2). At early times, both are dragged away with the flow $v < 0$ (towards the past) when effects of the subluminal dispersion of Eq. (4) dominate in F . As a result, the characteristic with positive has a turning point at $x_{\text{tp}}(\omega)$ of Eq. (6).

WKB approximation (in p -space) because it is valid when $\kappa/\Lambda \ll 1$, which we assume to be satisfied. Moreover, we restrict ourselves to $\omega/\Lambda \ll 1$ because it allows us to work in the *weak dispersive regime*, where $F(p) \sim p - p^3/(2\Lambda^2)$ offers a good approximation. Doing so, we obtain

$$\tilde{\phi}_\omega(p) = \frac{p^{-i\frac{\omega}{\kappa}}}{\sqrt{2\pi p F(p)}} \exp\left(-i\frac{p^3}{6\Lambda^2 \kappa}\right). \quad (9)$$

From the exponential factor, we see that the stationary modes involve a second composite length,

$$d_{\text{br}} = \frac{1}{(2\kappa)^{1/3} \Lambda^{2/3}}. \quad (10)$$

As we shall see below, d_{br} plays a prevalent role with respect to the ω -dependent length of Eq. (6).

INVERSE FOURIER ANALYSIS

To get the spatial properties of the mode, one should compute the inverse Fourier transform of Eq. (9). One then notices that the various solutions of Eq. (5) are recovered by adopting different contours \mathcal{C} in the complex p plane [6, 11–13, 17]

$$\phi_\omega^{\mathcal{C}}(x) = \int_{\mathcal{C}} \exp\left[i\left(q\frac{x}{d_{\text{br}}} - \frac{\omega}{\kappa} \ln(q) - \frac{1}{3}q^3\right)\right] \frac{dq}{2\pi q}. \quad (11)$$

To get this expression, we introduced the adimensionalized wave vector $q \doteq p d_{\text{br}}$. Irrespectively of the contour

\mathcal{C} and the value of ω , we see that $\phi_\omega(x)$ only depends on the adimensional distance $z \doteq x/d_{\text{br}}$. It should be pointed out that to get this result, we simplified the integrand of Eq. (11) by replacing $F(p)$ by p in the amplitude of Eq. (9). This is legitimate in the weak dispersive regime. Indeed, the prefactor modulates ϕ_ω on scales $|x| \gtrsim 1/\kappa$. Hence it is irrelevant for our near horizon analysis which is limited to $|z| = O(1)$, or $|x| \sim d_{\text{br}}$. For the expressions of the modulation, we refer to Sec.II.A of [11].

When choosing the contour \mathcal{C} , one should pay attention to the location of the branch cut of $\ln(q)$ which contains the only dependence in ω/κ . Here we shall only analyze the mode that decays inside the horizon. To obtain it, one must integrate on the contour defined in Fig.2. The mode so defined is proportional to the globally defined positive norm outgoing mode ϕ_ω^{out} .² Using the method

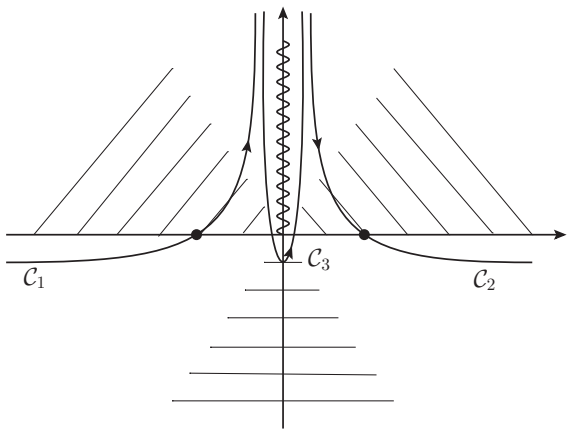


Figure 2. Contour of integration of Eq. (11) in the complex p -plane. \mathcal{C}_1 and \mathcal{C}_2 are evaluated by a saddle point approximation ($\pm p_{\text{saddle}}$ are indicated by black dots) and gives the outgoing branches, while \mathcal{C}_3 is obtained by setting $\Lambda \rightarrow \infty$, and gives the incoming branch (see Sec.II.A of [11] for a detailed derivation).

sketched in Fig.2, for $x > 0$ and $z = x/d_{\text{br}} \gg 1$, we obtain

$$\begin{aligned} \phi_\omega^{\mathcal{C}}(x) &\sim e^{-i\frac{\pi}{4}} \frac{e^{i\frac{2}{3}z^{3/2}} e^{-i\frac{\omega}{2\kappa} \ln z}}{\sqrt{4\pi z^{3/2}}} \\ &- \frac{\beta_\omega}{\alpha_\omega} e^{i\frac{\pi}{4}} \frac{e^{-i\frac{2}{3}z^{3/2}} e^{-i\frac{\omega}{2\kappa} \ln z}}{\sqrt{4\pi z^{3/2}}} \\ &+ \frac{1}{\alpha_\omega} z^{i\frac{\omega}{\kappa}} \sqrt{\frac{\kappa}{2\pi\omega}}. \end{aligned} \quad (12)$$

² It is interesting to notice that this mode was studied in the recent experiments based on surface waves in flume [19, 20]. This means that our forthcoming equations contain predictions that can be experimentally tested in a near future.

α_ω and β_ω are the Bogoliubov coefficients encoding the Hawking effect. Their ratio here obeys

$$\beta_\omega = e^{-\frac{\pi\omega}{\kappa}} \alpha_\omega, \quad (13)$$

as in the relativistic case. Thus, the temperature is still given by the standard expression $T_H = \kappa/2\pi$. On the other side of the horizon ($x < 0$), the mode decays as

$$\phi_\omega^{\mathcal{C}}(x) \sim e^{i\frac{\pi}{2}} e^{-\frac{\omega}{2\kappa}} \frac{e^{-\frac{2}{3}|z|^{3/2}} e^{-i\frac{\omega}{2\kappa} \ln |z|}}{\sqrt{4\pi |z|^{3/2}}}. \quad (14)$$

In this we recover that the corresponding characteristic with $\omega > 0$ bounces off without crossing the horizon, see Fig. 1.

It should now be stressed that these results are valid for $|x|$ large enough. More precisely, they require

$$|x| \gg d_{\text{br}}, \quad (15a)$$

$$|x| \gg x_{\text{tp}}. \quad (15b)$$

However, they also require $|x| \lesssim x_{\text{lin}}$, since $v \sim -1 + \kappa x$ has been used. When Λ/κ is large enough, the spatial range satisfying these three inequalities is quite large. For frequencies $\omega/\kappa \ll 1$, one has $x_{\text{tp}} \ll d_{\text{br}}$. Hence Eq. (15a) implies Eq. (15b). For $\omega \gg \kappa$, one has instead $x_{\text{tp}} \gg d_{\text{br}}$. However, the Hawking process is then exponentially suppressed. Therefore, (15a) is the most relevant condition to accurately obtain the connection formulae.

Further away from the horizon, the 4 modes are well approximated by a WKB approximation (in x -space) under the condition, see App.A of [11],

$$\left| \frac{\partial_x \ln[F(p_\omega)v_g(p_\omega)]}{p_\omega} \right| \ll 1. \quad (16)$$

Far from the horizon, this gives $|\partial_x v/\omega| \ll 1$ for the low momentum mode. For high momentum, one gets $|\partial_x v/\Lambda| \ll 1$ which is very well satisfied since $\kappa/\Lambda \ll 1$. As a result, short wavelength modes freely propagate. Therefore, the relativistic limit $\Lambda \rightarrow \infty$ in Eq. (5) can be taken safely, and the residual scattering can be obtained using the relativistic equation.

We thus conclude that the total S -matrix factorizes

$$S = \underbrace{\begin{pmatrix} 1 & 0 & 0 \\ 0 & \alpha_\omega^{\text{int}*} & \beta_\omega^{\text{int}*} \\ 0 & \beta_\omega^{\text{int}} & \alpha_\omega^{\text{int}} \end{pmatrix}}_{\text{inside scattering}} \cdot \underbrace{\begin{pmatrix} T_\omega & 0 & R_\omega \\ 0 & 1 & 0 \\ \tilde{R}_\omega & 0 & \tilde{T}_\omega \end{pmatrix}}_{\text{outside scattering}} \cdot \underbrace{\begin{pmatrix} \alpha_\omega & \beta_\omega & 0 \\ \tilde{\beta}_\omega & \tilde{\alpha}_\omega & 0 \\ 0 & 0 & 1 \end{pmatrix}}_{\text{near horizon scattering}}. \quad (17)$$

The two matrices on the left describe the late time, low momentum, scatterings that can be evaluated using the relativistic equation. The first one describes the mixing of the spectator infalling mode with the partner mode. It is an element of $U(1, 1)$ since these have opposite norms. The second matrix encodes the elastic mode mixing in

the outside region and gives the so-called greybody factors [21]. The third matrix on the right describes the early, high momentum, scattering. In the weak dispersive regime, Eq. (12) fixes the norm of the scattering coefficients $|\tilde{\beta}_\omega/\tilde{\alpha}_\omega|^2 = |\beta_\omega/\alpha_\omega|^2 = e^{-2\pi\omega/\kappa}$.

However, because of Eq. (15a), Eq. (12) says nothing about the mode behavior in a close vicinity of the horizon. Performing exactly the integral in Eq. (11), as done in [17], one finds that this behavior is given in terms of sums of hypergeometric functions ${}_1F_2$. Because the exact expressions are cumbersome³, in what follows, we separately analyze Eq. (11) for low and high frequency. Two distinct regimes clearly appear.

Small frequency regime $\omega \lesssim T_H$

In the limit $\omega \rightarrow 0$, we get

$$\phi_0^{\mathcal{C}}(x) = \int_C \exp\left(\frac{iqx}{d_{\text{br}}} - \frac{iq^3}{3}\right) \frac{dq}{2\pi q}. \quad (18)$$

For the contour of Fig.2, Eq. (18) is proportional the *primitive integral* of the Airy function $\text{Ai}(z)$ that vanishes for $x \rightarrow -\infty$, see [22]. Calling it $\text{PAi}(z)$, we get

$$\phi_0^{\mathcal{C}}(x) = i\text{PAi}\left(-\frac{x}{d_{\text{br}}}\right). \quad (19)$$

This result is consistent with Eq. (12). Indeed, for $\omega \ll T_H$, using $\beta_\omega \sim \alpha_\omega$, Eq. (12) becomes

$$\phi_0^{\mathcal{C}}(x) = i \frac{\sin[2/3(x/d_{\text{br}})^{3/2} - \pi/4]}{\sqrt{\pi(x/d_{\text{br}})^{3/2}}} + i, \quad (20)$$

which is the large z approximation of Eq. (19). In white hole flows, this mode gives the spatial profile of the *undulation* studied in [23, 24], and observed in [25].

For non-zero $\omega \lesssim T_H$, the first effect implied by Eq. (12) is a modulation of the profile (20) by $\exp(i\omega/2\kappa \ln[x/d_{\text{br}}])$. The location of the first node is given by $x_{\text{zero}} \sim d_{\text{br}} e^{4\pi\kappa/\omega}$. For $\omega \sim T_H$, we thus have $x_{\text{zero}}/d_{\text{br}} \sim e^{8\pi^2}$. Hence, this modulation possesses a wavelength much larger than d_{br} , possibly even larger than the near horizon size x_{lin} . We conclude that it is a subdominant effect, barely visible as long as $\omega \lesssim T_H$. As a result, the first significant effect comes from the $\beta_\omega/\alpha_\omega$ factor. To study it, we decompose the mode in its real and imaginary parts

$$\phi_\omega^{\mathcal{C}}(x) = i \frac{1 + e^{-\frac{\pi\omega}{\kappa}}}{2} \varphi_\omega(x) + \frac{1 - e^{-\frac{\pi\omega}{\kappa}}}{2} \psi_\omega(x), \quad (21)$$

³ Note also that the integrand of Eq. (11) in [17] differs from ours in several respects.

where φ_ω and ψ_ω are *real* functions. To lowest order in ω/κ , φ_ω reduces to Eq. (19). Similarly, ψ_ω is also independent of ω . This is neatly confirmed in Fig.3. The spatial properties of $\psi_{\omega \rightarrow 0}$ follow from the fact that ψ_0 obeys $-\partial_z^3 \psi_0 - z \partial_z \psi_0 = \phi_0^{\mathcal{C}}(z)$. Its spatial behavior is thus similar to that of Airy functions.

In conclusion, Eqs. (19), (21), and Fig. 3 explicitly give the near horizon properties of dispersive modes for *several* d_{br} lengths, and for all frequencies in the domain $0 \leq \omega \lesssim 3T_H$, which is the most relevant domain for the Hawking effect. This is our principal result.

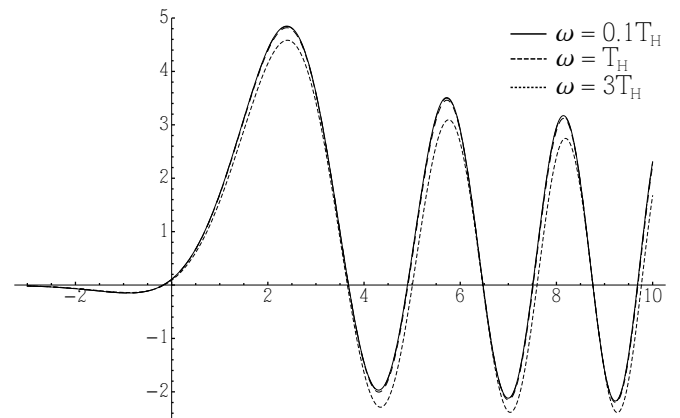


Figure 3. Plot of $-\partial_x \psi_\omega(z d_{\text{br}})$ of Eq. (21) as a function of z , i.e. we work in units of d_{br} , for $\Lambda/\kappa = 20$ and with four values of ω . For numerical reasons, we plotted the derivative instead of ψ_ω itself. Only the curve for $\omega = 3T_H$ (dashed line) can be distinguished from the others. This establishes that Eq. (21) offers an accurate description of the near horizon profile for several d_{br} lengths, and for $\omega \lesssim 3T_H$.

Large frequency regime $\omega \gg T_H$

To complete the picture, it is worth examining what happens at large frequencies. When ω is larger than T_H , the β_ω -term in Eq. (12) is exponentially small. The anomalous mode mixing is thus progressively turned off, and one is left with a total reflection. To obtain the mode near the turning point, we now follow the standard procedure. It consists in expanding the phase of the integrand of Eq. (11), i.e., $W(z, q) = zq - \frac{\omega}{\kappa} \ln(q) - \frac{1}{3}q^3$, to third order in $\Delta q = q - q_{\text{tp}}$, where $q_{\text{tp}}(\omega) = d_{\text{br}} p_{\text{tp}}$ is the adimensionalized momentum at the turning point. Performing the q -integration, by construction, one obtains an Airy function:

$$\phi_\omega^{\mathcal{C}}(x) = \frac{e^{i\theta_{\text{tp}}}}{3^{1/3} q_{\text{tp}}} e^{izq_{\text{tp}}} \text{Ai}\left(-\frac{z - z_{\text{tp}}}{3^{1/3}}\right), \quad (22)$$

where $z_{\text{tp}} = x_{\text{tp}}/d_{\text{br}}$, see Eq. (6), and where $\theta_{\text{tp}} = -\omega/(3\kappa) \ln(\omega/2\kappa) - \omega/(6\kappa)$. Eq. (22) is valid as long as

$|\Delta q| \ll |\partial_q^3 W / \partial_q^4 W|$. Moreover, the range of Δq should be at least of order 1 since one must integrate on several oscillations of e^{iq^3} to accurately get an Airy function. Therefore, the inequality becomes

$$\left| \frac{\partial_q^4 W}{\partial_q^3 W} \right| \sim \left| \frac{1}{q_{\text{tp}}} \right| \sim \left| \frac{1}{d_{\text{br}} p_{\text{tp}}} \right| \sim \left| \frac{2\kappa}{\omega} \right|^{1/3} \ll 1. \quad (23)$$

The inequality $|\Delta q| \ll \left| \frac{2\kappa}{\omega} \right|^{-1/3}$ also restricts the validity range of z of Eq. (22). Indeed, for $\Delta z \gtrsim 1$, the values of q that mainly contributes to the integral (11) are around the saddle point, which increases as $\Delta z^{1/2} = |z - z_{\text{tp}}|^{1/2}$. It implies that $\phi_\omega(x)$ is correctly approximated by Eq. (22) only for $\Delta z \ll q_{\text{tp}}^2$, i.e., $|x - x_{\text{tp}}| \ll x_{\text{tp}}$. Yet, such interval can contain several d_{br} lengths since we work at large ω/κ . This is confirmed in Fig. 4. As can be seen, Eq. (22) is valid for larger ranges of $z = x/d_{\text{br}}$ when ω/κ increases.

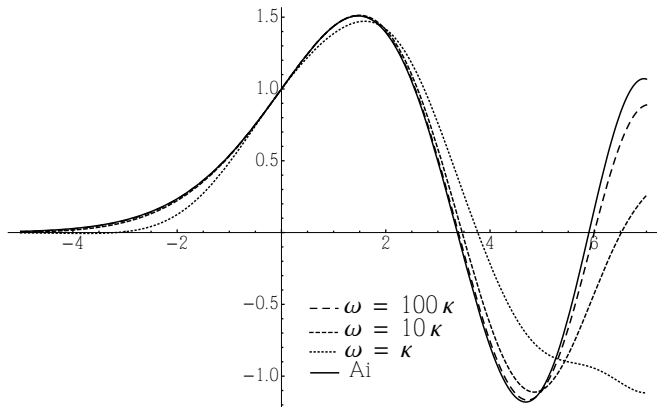


Figure 4. Plot of $e^{-izq_{\text{tp}}} \times \phi_\omega^C(x_{\text{tp}} + zd_{\text{br}})$ as a function of z , for $\Lambda/\kappa = 20$, various values of ω , and also compared with the Airy function $\text{Ai}(-z/3^{1/3})$. The different curves are normalized to 1 at the turning point $z_{\text{tp}}(\omega)$, which is here set at $z = 0$. When ω increases, the matching with the Airy function gets better, and for a larger range of z . By numerically comparing the values at the first peak, we found that the error decreases as $\sim (\kappa/\omega)^\gamma$ with the exponent $1/3.25 \lesssim \gamma \lesssim 1/3.15$, in agreement with Eq. (23) to a good accuracy. Notice that since we factorized $e^{izq_{\text{tp}}}$, Eq. (22) is valid for many short wave lengths oscillations controlled by q_{tp} .

We also point out that Eq. (22) is rapidly modulated by a high wave number p_{tp} , and that the Airy function gives the slowly varying envelope [26]. This scale separation follows from Eq. (23) which implies $p_{\text{tp}} \gg 1/d_{\text{br}}$. Hence, for $\omega \gg T_H$, ϕ_ω and $\partial_x \phi_\omega$ are both described by Airy functions. This contrasts with the low frequency regime where there is no rapid modulation, and where only $\partial_x \phi_\omega$ is described by the Airy function Ai . At low ω/κ , the profile of ϕ_ω has thus a phase shift of $\pi/2$ with respect to that of the Ai function. This phase shift could be experimentally validated.

In conclusion of this Section, it should be emphasized that Eq. (23) implies that Eq. (22) offers a good approximation only when the Hawking effect is negligible, $\beta_\omega \ll 1$. This can be understood by noticing that we integrated only over positive values of p centered around p_{tp} . The contribution of negative p , which is responsible for $\beta_\omega \neq 0$, has thus been neglected. As a byproduct, the notion of “ ω -dependent group velocity horizon” (i.e., the turning point of Eq. (6)) is not relevant for the Hawking effect. Indeed, x_{tp} can be distinguished from the Killing horizon at $x = 0$ only if they are distant by several broadening lengths d_{br} , i.e.

$$\frac{x_{\text{tp}}}{d_{\text{br}}} \sim \left(\frac{\omega}{\kappa} \right)^{2/3} \gg 1, \quad (24)$$

which is satisfied only when the Hawking radiation is exponentially suppressed.

SMOOTHING OUT SHORT-DISTANCE DETAILS

When computing the corrections to the Hawking spectrum due to dispersion, it is a priori tempting to take into account the ω -dependence of Eq. (6). In particular, to optimize the calculation of the spectrum, one could have used the local value of the gradient [27, 28] $\kappa_{\text{tp}}(\omega) = \partial_x v(x_{\text{tp}}(\omega))$ in the place of κ_{hor} evaluated at the Killing horizon. Yet, no such dependence was found in numerical analysis of the spectrum [14, 15].

This lack of dependence is corroborated by the above study of near horizon modes which indicates that the best fit for the effective surface gravity should be obtained by averaging $\partial_x v$ over a broadening length. This is because the finite resolution of the modes will erase the details of the background on scales smaller than d_{br} . In this we recover what was numerically observed in [15]. To clarify this, we consider a background profile separated in two contributions $v(x) = v_0(x) + \delta v(x)$, where v_0 is smooth enough so that the approximations used above work, and where δv is a small amplitude perturbation. If this amplitude is small enough, adapting the *distorted wave Born approximation* [29] to anomalous scattering, we can evaluate the induced correction of the Bogoliubov coefficient. This gives

$$\delta\beta_\omega = 2i\pi \int [\phi_{-\omega}^{\text{out}} \partial_x (\delta v \pi_\omega^{\text{in}}) + \pi_{-\omega}^{\text{out}} \delta v \partial_x \phi_\omega^{\text{in}}] dx, \quad (25)$$

where $\pi(x)$ is the conjugate momentum of ϕ given by $\pi = (\partial_t + v\partial_x)\phi$, and where ϕ_ω^{in} (ϕ_ω^{out}) designates the incoming (outgoing) positive norm mode of frequency ω propagating in the unperturbed flow. From this expression, we clearly see that if the spatial scale of variation of δv is much shorter than d_{br} , the integral is automatically smoothed out. As a result, $\delta\beta_\omega$ will essentially vanish.

CONCLUSION

Our main conclusion is that in dispersive theories, event horizons effectively acquire a finite spatial extension given by d_{br} of Eq. (10). We reached this by analyzing the spatial properties of the stationary modes in the near horizon region, and by showing that they are smoothed out on that scale, irrespectively of their frequency. These properties explain that, when the velocity gradient (surface gravity) does not significantly vary over that scale, Hawking radiation is recovered and the S -matrix factorizes according to Eq. (17). In addition, we established that the usual WKB resolution near a turning point becomes valid for high frequencies, precisely in the regime where the Hawking process is negligible.

* antonin.coutant@aei.mpg.de

† renaud.parentani@th.u-psud.fr

- [1] W. G. Unruh, “Notes on black-hole evaporation,” *Phys. Rev. D* **14** no. 4, (1976) 870–892.
- [2] S. Hawking, “Black hole explosions,” *Nature* **248** (1974) 30–31.
- [3] T. Damour and R. Ruffini, “Black Hole Evaporation in the Klein-Sauter-Heisenberg-Euler Formalism,” *Phys. Rev. D* **14** (1976) 332–334.
- [4] R. Brout, S. Massar, R. Parentani, and P. Spindel, “A Primer for black hole quantum physics,” *Phys. Rept.* **260** (1995) 329–454, [arXiv:0710.4345 \[gr-qc\]](#).
- [5] W. Unruh, “Sonic analog of black holes and the effects of high frequencies on black hole evaporation,” *Phys. Rev. D* **51** (1995) 2827–2838.
- [6] R. Brout, S. Massar, R. Parentani, and P. Spindel, “Hawking radiation without transPlanckian frequencies,” *Phys. Rev. D* **52** (1995) 4559–4568, [arXiv:hep-th/9506121 \[hep-th\]](#).
- [7] T. Jacobson, “Black hole evaporation and ultrashort distances,” *Phys. Rev. D* **44** (1991) 1731–1739.
- [8] T. Jacobson, “Trans Planckian redshifts and the substance of the space-time river,” *Prog. Theor. Phys. Suppl.* **136** (1999) 1–17, [arXiv:hep-th/0001085 \[hep-th\]](#).
- [9] R. Balbinot, A. Fabbri, S. Fagnocchi, and R. Parentani, “Hawking radiation from acoustic black holes, short distance and back-reaction effects,” *Riv. Nuovo Cim.* **28** (2005) 1–55, [arXiv:gr-qc/0601079 \[gr-qc\]](#).
- [10] C. Barcelo, S. Liberati, and M. Visser, “Analogue gravity,” *Living Rev. Rel.* **8** (2005) 12, [arXiv:gr-qc/0505065 \[gr-qc\]](#).
- [11] A. Coutant, R. Parentani, and S. Finazzi, “Black hole radiation with short distance dispersion, an analytical S -matrix approach,” *Phys. Rev. D* **85** (2012) 024021, [arXiv:1108.1821 \[hep-th\]](#).
- [12] S. Corley, “Computing the spectrum of black hole radiation in the presence of high frequency dispersion: An Analytical approach,” *Phys. Rev. D* **57** (1998) 6280–6291, [arXiv:hep-th/9710075 \[hep-th\]](#).
- [13] W. G. Unruh and R. Schutzhold, “On the universality of the Hawking effect,” *Phys. Rev. D* **71** (2005) 024028, [arXiv:gr-qc/0408009 \[gr-qc\]](#).
- [14] J. Macher and R. Parentani, “Black/White hole radiation from dispersive theories,” *Phys. Rev. D* **79** (2009) 124008, [arXiv:0903.2224 \[hep-th\]](#).
- [15] S. Finazzi and R. Parentani, “Spectral properties of acoustic black hole radiation: broadening the horizon,” *Phys. Rev. D* **83** (2011) 084010, [arXiv:1012.1556 \[gr-qc\]](#).
- [16] S. Finazzi and R. Parentani, “Hawking radiation in dispersive theories, the two regimes,” *Phys. Rev. D* **85** (2012) 124027, [arXiv:1202.6015 \[gr-qc\]](#).
- [17] V. Fleurov and R. Schilling, “Regularization of fluctuations near the sonic horizon due to the quantum potential and its influence on Hawking radiation,” *Phys. Rev. A* **85** (2012) 045602, [arXiv:1105.0799 \[cond-mat.quant-gas\]](#).
- [18] X. Busch and R. Parentani, “Dispersive fields in de Sitter space and event horizon thermodynamics,” *Phys. Rev. D* **86** (2012) 104033, [arXiv:1207.5961 \[hep-th\]](#).
- [19] G. Rousseaux, C. Mathis, P. Maissa, T. G. Philbin, and U. Leonhardt, “Observation of negative phase velocity waves in a water tank: A classical analogue to the Hawking effect?,” *New J. Phys.* **10** (2008) 053015, [arXiv:0711.4767 \[gr-qc\]](#).
- [20] S. Weinfurter, E. W. Tedford, M. C. Penrice, W. G. Unruh, and G. A. Lawrence, “Measurement of stimulated Hawking emission in an analogue system,” *Phys. Rev. Lett.* **106** (2011) 021302, [arXiv:1008.1911 \[gr-qc\]](#).
- [21] D. N. Page, “Particle Emission Rates from a Black Hole: Massless Particles from an Uncharged, Nonrotating Hole,” *Phys. Rev. D* **13** (1976) 198–206.
- [22] M. Abramowitz and I. Stegun, *Handbook of mathematical functions with formulas, graphs, and mathematical tables*, vol. 55. Dover publications, 1964.
- [23] A. Coutant and R. Parentani, “Undulations from amplified low frequency surface waves,” [arXiv:1211.2001 \[physics.flu-dyn\]](#).
- [24] C. Mayoral, A. Recati, A. Fabbri, R. Parentani, R. Balbinot, and I. Carusotto, “Acoustic white holes in flowing atomic Bose-Einstein condensates,” *New J. Phys.* **13** (2011) 025007, [arXiv:1009.6196 \[cond-mat.quant-gas\]](#).
- [25] S. Weinfurter, E. W. Tedford, M. C. Penrice, W. G. Unruh, and G. A. Lawrence, “Classical aspects of Hawking radiation verified in analogue gravity experiment,” [arXiv:1302.0375 \[gr-qc\]](#).
- [26] J.-C. Nardin, G. Rousseaux, and P. Couillet, “Wave-Current Interaction as a Spatial Dynamical System: Analogies with Rainbow and Black Hole Physics,” *Phys. Rev. Lett.* **102** (2009) 124504.
- [27] S. Corley and T. Jacobson, “Hawking spectrum and high frequency dispersion,” *Phys. Rev. D* **54** (1996) 1568–1586, [arXiv:hep-th/9601073 \[hep-th\]](#).
- [28] R. Schutzhold and W. G. Unruh, “On the origin of the particles in black hole evaporation,” *Phys. Rev. D* **78** (2008) 041504, [arXiv:0804.1686 \[gr-qc\]](#).
- [29] R. G. Newton, *Scattering theory of waves and particles*. Courier Dover Publications, 1982.